Article:
Molz, Barbara, Herbik, Anne, Baseler, Heidi orcid.org/0000-0003-0995-8453 et al. (18 more authors) (2021) Structural changes to primary visual cortex in the congenital absence of cone input in achromatopsia. NeuroImage: Clinical. 102925. ISSN 2213-1582

https://doi.org/10.1016/j.nicl.2021.102925

NeuroImage: Clinical 33 (2022) 102925

Contents lists available at ScienceDirect

NeuroImage: Clinical

journal homepage: www.elsevier.com/locate/ynicl

Structural changes to primary visual cortex in the congenital absence of cone input in achromatopsia

Barbara Molz [a,b,1], Anne Herbik [c], Heidi A. Baseler [a,d,e,1], Pieter B. de Best [f,1], Richard W. Vernon [a], Noa Raz [f,1], Andre D. Gouws [g,1], Khazar Ahmadi [c,1], Rebecca Lowndes [g], Rebecca J. McLean [h], Irene Gottlob [h], Susanne Kohl [i], Lars Choritz [c], John Maguire [j], Martin Kanowski [k], Barbara Käsmann-Kellner [l], Ilse Wieland [m], Eyal Banin [n], Netta Levin [f,1,2], Michael B. Hoffmann [c,o,1,2], Antony B. Morland [a,e,g,1,2,*]

[a] Department of Psychology, University of York, Heslington, YO10 5DD York, United Kingdom
[b] Language and Genetics Department, Max Planck Institute for Psycholinguistics, 6525 XD Nijmegen, Netherlands
[c] Department of Ophthalmology, University Hospital, Otto-von-Guericke University, 39120 Magdeburg, Germany
[d] Hull York Medical School, University of York, Heslington, YO10 5DD York, United Kingdom
[e] York Biomedical Research Institute, University of York, Heslington, YO10 5DD York, United Kingdom
[f] MRI Unit, Department of Neurology, Hadassah Medical Center, 91120 Jerusalem, Israel
[g] York Neuroimaging Centre, Department of Psychology, University of York, YO10 5NY York, United Kingdom
[h] University of Leicester Ulverscroft Eye Unit, University of Leicester, Leicester Royal Infirmary, LE2 7LX Leicester, United Kingdom
[i] Molecular Genetics Laboratory, Institute for Ophthalmic Research, Centre for Ophthalmology, University Clinics Tübingen, 72076 Tübingen, Germany
[j] School of Optometry and Vision Sciences, University of Bradford, BD7 1DP Bradford, United Kingdom
[k] Department of Neurology, University Hospital, Otto-von-Guericke University, 39120 Magdeburg, Germany
[l] Department of Ophthalmology, Saarland University Hospital and Medical Faculty of the Saarland University, 66421 Homburg, Germany
[m] Department for Molecular Genetics, Institute for Human Genetics, University Hospital, Otto-von-Guericke University, 39120 Magdeburg, Germany
[n] Degenerative Diseases of the Retina Unit, Department of Ophthalmology, Hadassah Medical Center, 91120 Jerusalem, Israel
[o] Center for Behavioral Brain Sciences, 39106 Magdeburg, Germany

ARTICLE INFO

Keywords:
Achromatopsia
sMRI
Surface-based morphology
Plasticity
Primary visual cortex

ABSTRACT

Autosomal recessive Achromatopsia (ACHM) is a rare inherited disorder associated with dysfunctional cone photoreceptors resulting in a congenital absence of cone input to visual cortex. This might lead to distinct changes in cortical architecture with a negative impact on the success of gene augmentation therapies. To investigate the status of the visual cortex in these patients, we performed a multi-centre study focusing on the cortical structure of regions that normally receive predominantly cone input. Using high-resolution T1-weighted MRI scans and surface-based morphometry, we compared cortical thickness, surface area and grey matter volume in foveal, parafoveal and paracentral representations of primary visual cortex in 15 individuals with ACHM and 42 normally sighted, healthy controls (HC). In ACHM, surface area was reduced in all tested representations, while thickening of the cortex was found highly localized to the most central representation. These results were comparable to more widespread changes in brain structure reported in congenitally blind individuals, suggesting similar developmental processes, i.e., irrespective of the underlying cause and extent of vision loss. The cortical differences we report here could limit the success of treatment of ACHM in adulthood. Interventions earlier in life when cortical structure is not different from normal would likely offer better visual outcomes for those with ACHM.

* Corresponding author at: Department of Psychology, University of York, Heslington, YO10 5DD York, United Kingdom.
E-mail address: antony.morland@york.ac.uk (A.B. Morland).
[1] NextGenVis-consortium members.
[2] These authors contributed equally to this work.

https://doi.org/10.1016/j.nicl.2021.102925
Received 7 August 2021; Received in revised form 20 December 2021; Accepted 21 December 2021
Available online 21 December 2021

1. Introduction

With the rise of gene therapeutic interventions to treat congenital ophthalmological diseases, assessing the structural integrity of visual cortex is critical as successful visual rehabilitation will ultimately rely on intact brain function. Achromatopsia (ACHM), a rare (1:30,000) monogenic, autosomal recessive visual disorder that affects signal transduction in cone photoreceptors (Aboshiha et al., 2016; Michalakis et al., 2017; Zobor et al., 2015), is currently the target of gene-addition therapy in a number of clinical trials (NCT03758404, NCT03001310, NCT03278873, NCT02935517, NCT02599922, NCT02610582, (Fischer et al., 2020)).

As cones are the only photoreceptors to occupy the central foveal region of the retina, patients with ACHM have a central scotoma and therefore reduced visual acuity from birth, along with an absence of colour vision, photophobia, hemeralopia and nystagmus (Haegerstrom-Portnoy et al., 1996; Remmer et al., 2015; Zobor et al., 2015). While the overall stationary or very slow progressing disease phenotype (Zobor et al., 2015) would generally be favourable for therapeutic intervention at any point during the lifespan in ACHM (Hirji et al., 2018) the way in which cortical structure develops during extended periods of cortical deprivation of cone inputs has not yet been assessed.

It is plausible that structural remodelling of the visual cortex due to lack of input may limit the processing of restored signals from the eye. Structural differences in the visual cortex have been reported in congenital visual disorders such as congenital anophthalmia, congenital glaucoma, albinism and retinitis pigmentosa (Bridge et al., 2014, 2009; Jiang et al., 2009; Park et al., 2009). Several studies using voxel-based morphometry (VBM) reported reduced grey matter volume in early blind individuals (Noppeney et al., 2005; Pan et al., 2007; Park et al., 2009; Ptito et al., 2008; Von Dem Hagen et al., 2005). Further studies applied a surface-based approach and linked the volumetric reduction to a decrease in surface area (Aguirre et al., 2016; Jiang et al., 2009; Park et al., 2009). Reductions in cortical volume and surface area were attributed in part to the loss of input to visual cortex early in life (Jiang et al., 2009; Park et al., 2009; Ptito et al., 2008). Independently, and perhaps counterintuitively however, a number of studies also found increased cortical thickness, e.g. in Leber congenital amaurosis (Aguirre et al., 2017), congenital anophthalmia (Bridge et al., 2009), Leber's hereditary optic neuropathy (d'Almeida et al., 2013) and other forms of congenital blindness (Aguirre et al., 2016; Anurova et al., 2015; Jiang et al., 2009; Park et al., 2009). Although the exact mechanisms behind these cortical changes have not yet been proven, there is evidence that they may indicate some form of neuronal degeneration or reorganization which could limit the outcome of vision restoration treatments (Guerreiro et al., 2016, 2015; Lemos et al., 2016; Prins et al., 2016a).

Understanding whether ACHM specifically affects the morphology of brain regions that process central vision is therefore a crucial factor in evaluating the potential success of gene augmentation therapies in this patient population. We hypothesise that individuals with ACHM will show distinct changes in cortical anatomy particularly in central visual field representations of primary visual cortex that have been deprived of normal cone input throughout development. This detailed analysis of the first and largest visual representation in the human brain complements our previous analysis of a larger number of visual areas of the occipital lobe (Lowndes et al., 2021).

2. Materials and methods

2.1. Participants

Data used in this study were collected as part of a multicentre project at three scanner sites (University of York, UK ("UY"), Hadassah Medical Center, Jerusalem, IL ("HMC"), University of Magdeburg, DE ("UM")). All participants had to be eligible for the MRI procedures used. Healthy control participants (HC) were required to have normal or corrected-to-normal vision. Inclusion criteria for patients were: i) genetically confirmed ACHM (biallelic *CNGA3* or *CNGB3* mutations as specified in Table 1), and ii) electroretinographically confirmed absence of cone function according to the ISCEV standard for full-field clinical electroretinography (McCulloch et al., 2015). High resolution structural scans from 42 participants (mean ± SD age, 30.29 ± 9.72; 19 males) with normal or corrected-to-normal vision (HC) and 15 participants with ACHM (age mean ± SD, 36.2 ± 10.26; 9 males) were utilised in this study. Experimental protocols received approval from the site-specific ethics committees and were in accordance with the Declaration of Helsinki. A previous study analyzing the data from the same participants has been published (Lowndes et al., 2021). A larger number of occipital lobe visual areas were assessed in that work, but it did not test for anatomical changes in difference eccentricity representations – the key aspect of the work presented here.

2.2. Data acquisition

2.2.1. York

A single, high resolution, anatomical, T1-weighted scan (TR, 2500 ms; TE, 2.26 ms; TI, 900 ms; voxel size, 1 × 1 × 1 mm^3; flip angle, 7°;

Table 1
Participant demographics. Overview table summarising participant type, scanner site, age, sex, and genotype of participants with achromatopsia; (HC = healthy control, ACHM = Participant with achromatopsia; UY = University of York, UM = University of Magdeburg, HMC = Hadassah Medical Centre; m = male, f = female);

Participant	Sex	Scanner Site	Participant	Sex	Scanner Site	Genotype
HC	m	HMC	ACHM	m	HMC	*CNGA3*
HC	f	HMC	ACHM	m	HMC	*CNGA3*
HC	m	HMC	ACHM	m	HMC	*CNGA3*
HC	f	HMC	ACHM	f	HMC	*CNGA3*
HC	f	HMC	ACHM	f	HMC	*CNGA3*
HC	m	HMC	ACHM	m	HMC	*CNGA3*
HC	f	HMC	ACHM	m	UM	*CNGB3*
HC	m	HMC	ACHM	f	UM	*CNGA3*
HC	m	HMC	ACHM	f	UM	*CNGB3*
HC	f	HMC	ACHM	m	UM	*CNGB3*
HC	f	HMC	ACHM	m	UM	*CNGA3*
HC	f	HMC	ACHM	f	UY	*CNGB3*
HC	f	HMC	ACHM	m	UY	*CNGB3*
HC	f	HMC	ACHM	m	UY	*CNGA3*
HC	f	HMC	ACHM	f	UY	*CNGA3*
HC	f	HMC				
HC	f	HMC				
HC	m	HMC				
HC	m	HMC				
HC	m	HMC				
HC	f	HMC				
HC	f	HMC				
HC	m	HMC				
HC	m	HMC				
HC	m	UM				
HC	f	UM				
HC	m	UM				
HC	m	UM				
HC	f	UM				
HC	f	UM				
HC	f	UM				
HC	m	UM				
HC	f	UY				
HC	f	UY				
HC	m	UY				
HC	m	UY				
HC	f	UY				
HC	m	UY				
HC	f	UY				
HC	m	UY				
HC	f	UY				
HC	m	UY				

matrix size, 256 × 256 × 176) was acquired using a 64-channel head coil on a SIEMENS MAGNETOM Prisma 3 T scanner at the York Neuroimaging Centre (YNiC).

2.2.2. Jerusalem

A single, high resolution, anatomical, T1-weighted scan (TR, 2300 ms; TE, 2.98 ms; TI, 900 ms; voxel size, 1 × 1 × 1 mm^3; flip angle, 9°; matrix size, 256 × 256 × 160) was acquired using a 32-channel head coil on a SIEMENS MAGNETOM Skyra 3 T scanner at the Edmond & Lily Safra Center for Brain Sciences, Hebrew University of Jerusalem.

2.2.3. Magdeburg

A single, high resolution, anatomical, T1-weighted scan (TR, 2500 ms; TE, 2.82 ms; TI, 1100 ms; voxel size, 1 × 1 × 1 mm3; flip angle, 7°; matrix size, 256 × 256 × 192) was acquired using a 64-channel head coil on a SIEMENS MAGNETOM Prisma 3 T scanner at the University Hospital, Magdeburg, Germany.

2.2.4. Data pre-processing

Surface-based morphology analysis was performed using the Freesurfer analysis suite, Version 6.0 (http://surfer.nmr.mgh.harvard.edu/). Cortical reconstruction and volumetric segmentation of the T1-weighted scans were performed automatically using the 'recon_all' script, described in more detail elsewhere (Dale et al., 1999; Fischl et al., 1999). In brief, the process included the removal of non-brain tissue (Ségonne et al., 2004), automated Talairach transformation, intensity normalisation (Sled et al., 1998), tessellation of the grey/white matter and pial boundaries (grey/cerebrospinal fluid) including automated topology correction and surface deformation (Dale et al., 1999; Fischl et al., 1999; Ségonne et al., 2004). After cortical models were derived, the cortical surface was inflated and registered to a sphere (Fischl et al., 1999) and the surface parcellated according to gyral and sulcal structures (Desikan et al., 2006; Fischl et al., 2004).

The final surface reconstruction was inspected for potential cortical segmentation errors and, when necessary, manually corrected using the FreeView Visualisation GUI. All manually corrected reconstructions were rerun ('autoreconall2') utilising the edited brainmask.mgz files.

2.3. Data analysis

We applied a region of interest (ROI)-based approach to maximise the sensitivity of our analysis and compared differences between participants with ACHM and HC in three surface-based measures: mean cortical thickness (mm), surface area (mm^2) and cortical volume (mm^3).

All surface-based metrics were extracted directly within each individual's native space, and no further smoothing was applied.

Cortical thickness was measured as the shortest distance between each grey/white boundary vertex and the pial surface (white matter/cerebrospinal fluid boundary) and vice versa. The final value depicted the average of the two thickness values measured, and thickness values were then averaged across the ROI (Fischl and Dale, 2000). Surface area was measured by calculating the summed surface area across each ROI of each triangle of the surface mesh, the unit used to connect the cortical surface between each vertex. Cortical volume was computed as the sum of oblique truncated polyhedrons, as described in Winkler et al. (2018).

ROIs used for this analysis stream were derived using the anatomically defined retinotopy atlas ("benson14_retinotopy" command) implemented in the python analysis toolbox 'neuropythy' (Benson et al., 2014; Benson and Winawer, 2018). The atlas created several Freesurfer-based maps (visual area, eccentricity, polar angle, pRF size), which were

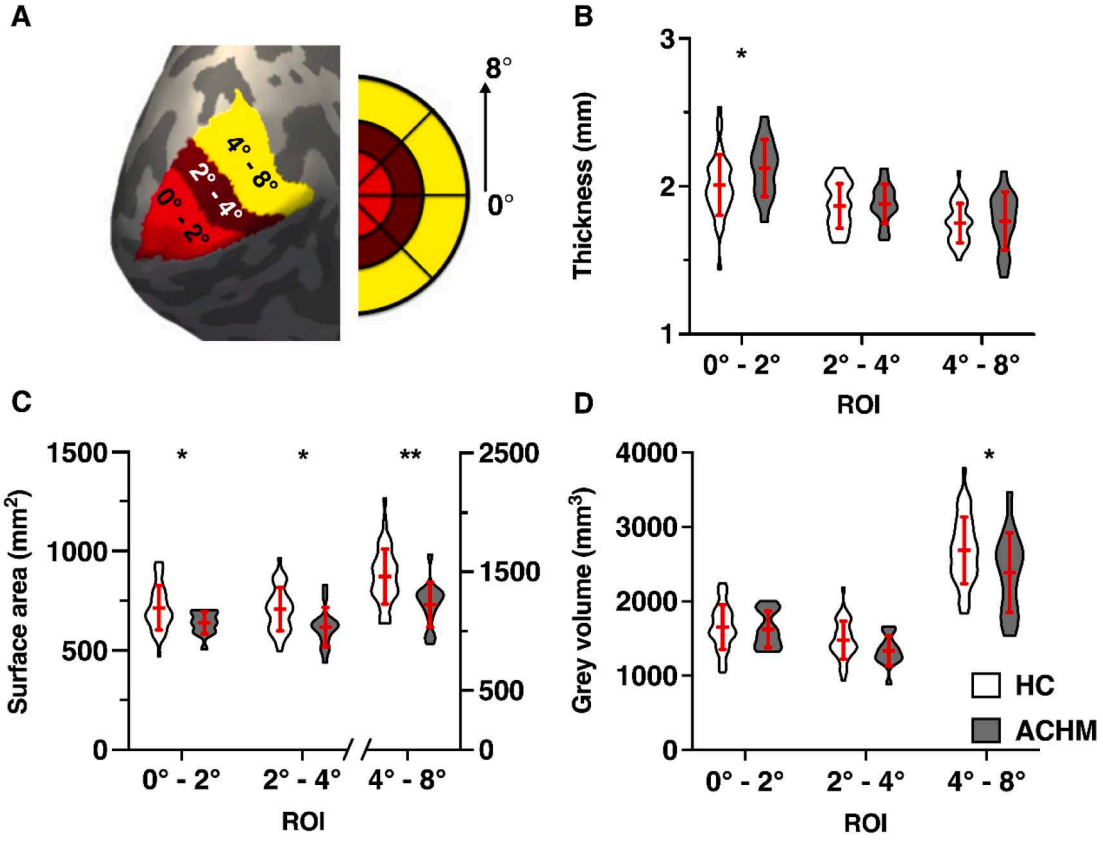

Fig. 1. ROI surface-based morphometric values (A) shows the left hemisphere cortical surface reconstruction of an example participant with the three overlaid ROI labels: ROI_{Fovea} (0°-2°), $ROI_{Parafovea}$ (2° −4°) and $ROI_{Paracentral}$ (4°-8°); violin plots show the mean cortical thickness (B), pooled surface area (C) and grey matter volume (D) in all ROIs for healthy control participants (HC, N = 42) and participants with achromatopsia (ACHM, N = 15); error bars represent +/- 1 standard deviation; *p < .05, **p < .01;

used to delineate three ROI labels for each participant in each hemisphere. The ROIs represented the foveal (0-2°), parafoveal (2-4°) and paracentral representations (4-8°) of V1 (Fig. 1A).

Extracted values were combined across both hemispheres, where surface area and cortical volume were simply summed for each participant. For cortical thickness, the values were weighted by the respective surface area value and the mean cortical thickness value derived via following calculation:

ThicknessTotal = ((lh.thickness * lh.surfacearea) + (rh.thickness * rh.surfacearea))/ (lh.surfacearea + rh.surfacearea).

2.4. Statistical analysis

All statistical analyses were performed in the IBM SPSS Statistics software package, version 25. Graphs were created using Prism version 8.00 for Mac (GraphPad Software, La Jolla California USA, www.graphpad.com).

A hierarchical linear regression was applied to assess the ability of each independent variable to predict the three outcome measures (cortical thickness, grey matter volume, cortical surface area) in each of our three ROIs for each participant group. Normality for each group/ROI was confirmed using the Shapiro-Wilks test and the P-P and scatter plot of the regression standardized residuals were inspected and conformed to the assumptions necessary for subsequent analyses. Neither age (Welch Two Sample *t*-test; $t = 1.94$, $df = 23.58$, $p = .064$) nor sex (χ^2 (1, $N = 57$) $= 0.46$, $p = .50$) were significantly different between the two cohorts. Nevertheless, we accounted for any variance explained by both sex and age, and as well as scanner site and global brain scaling (global mean thickness, global overall surface area and estimated intracranial volume) as they represent known confounding factors (Alfaro-Almagro et al., 2021). Therefore, these confounding variables were entered in the first step of the hierarchical linear regression model (Model 1), while participant group, our main variable of interest, (HC and ACHM) was added in the second analysis step (Model 2). This hierarchical model allowed us to determine if participant group (ACHM vs control) could explain a significant amount of the variance within our sample after accounting for the confounding factors added in Model 1. The effect of participant group would be reflected in a significant change in ΔR^2. Results were subsequently adjusted for multiple comparisons (three regions of interest) by applying the sequential Holm–Bonferroni correction (Holm, 1979) where the adjusted alpha levels, denoted as p_α, are reported for each comparison.

3. Results

We acquired high-resolution T1-weighted images from 15 genetically confirmed participants with ACHM and compared these to 42 normally sighted individuals scanned at each of the three sites, with demographics summarised in Table 1.

Fig. 1 displays the regions of interest analysed within primary visual cortex and compares cortical measures between HC and ACHM participant groups.

After accounting for any variance explained by our confounding variables (Table 2, Model 1), we first assessed the impact of absent cone input on cortical thickness (Table 2, Model 2). As shown in Figure 1B, a significant increase in cortical thickness was found in ACHM within the most foveal representation ($\Delta R^2 = 7.4\%$; ($F(1,50) = 6.173$, $p_{0.017} = 0.016$), while no increase in cortical thickness was seen within the parafoveal and paracentral representations of primary visual cortex in ACHM (2–4°: $\Delta R^2 = 0.1$ %; $F(1,50) = 0.046$, $p_{0.05} = 0.832$; 4–8°: $\Delta R^2 = 0.3\%$; $F(1,50) = 0.224$, $p_{0.025} = 0.638$).

Next, we compared surface area of each ROI between groups (Fig. 1C), and found that it was significantly reduced in ACHM across all ROIs, with the highest reduction found in the paracentral region (0–2°: $\Delta R^2 = 4.2$ %; $F(1,50) = 5.651$, $p_{0.025} = 0.021$; 2–4°: $\Delta R^2 = 5.5$ %; $F(1,50) = 4.846$, $p_{0.05} = 0.032$; 4–8°: $\Delta R^2 = 17.6\%$; $F(1,50) = 12.851$, $p_{0.017} = 0.001$).

Finally, we assessed grey matter volume. In contrast to surface area, grey matter volume was significantly reduced paracentrally but only when considering the unadjusted alpha level ($\Delta R^2 = 8.8\%$; $F(1,50) = 5.398$, $p_{0.017} = 0.024$), as depicted in Fig. 1D. In contrast, foveal and parafoveal representations of primary visual cortex showed no significant change in cortical grey matter volume (0–2°: $\Delta R^2 = 0$ %; $F(1,50) = 0.027$, $p_{0.05} = 0.871$; 2–4°: $\Delta R^2 = 3.7$ %; $F(1,50) = 3.167$, $p_{0.025} = 0.081$).

4. Discussion

We applied surface-based morphometry to analyse cortical structure in ACHM, a patient population with a congenital lack of cone function, resulting in a complete loss of input from the fovea. We employed a hierarchical regression analysis to determine any differences between ACHM and HC while accounting for the variance explained by various confounding variables. Our results reveal thicker primary visual cortex in the representations of the region of absolute loss of vision in these patients. We also found a more widespread reduction in the surface area of primary visual cortex within the central representation (0–8°) we assessed.

4.1. Cortical thickening localized to foveal visual field representations

The cortical thickening observed in the central visual field representation is consistent with that reported in several other studies of congenital total blindness. Critically, however, it is localised to the

Table 2
Summary of Hierarchical Regression Analysis. Mean values and standard deviation are denoted for each metric and ROI as well as F-values, degrees of freedom, associated p-values and for Model 2 also ΔR^2; ROI = region of interest, ACHM = Achromatopsia, HC = healthy control; Significant differences for each metric for confounding variables entered in Model 1 (combined variance explained by scanner site, age, sex, global brain metric) or Model 2 (predictor variable: participant group): * $p < .05$, ** $p < .01$, *** $p < .001$

Metric	ROI	ACHM		HC		Model 1			Model 2			
		M	SD	M	SD	F(5,51)	p-value		F(1,50)	ΔR^2	p-value	
Thickness (mm)	Fovea	2.12	0.19	2.01	0.21	4.966	0.001	**	6.173	0.074	0.016	*
	Parafovea	1.88	0.13	1.87	0.15	5.158	0.001	**	0.046	0.001	0.832	
	Paracentral	1.77	0.20	1.75	0.13	2.837	0.025	*	0.224	0.003	0.638	
Surface area (mm^2)	Fovea	639.00	55.84	713.29	111.39	14.508	> 0.001	***	5.651	0.042	0.021	*
	Parafovea	616.67	98.57	706.62	109.26	6.194	> 0.001	***	4.846	0.055	0.032	*
	Paracentral	1224.67	189.24	1462.71	232.01	1.633	0.168		12.851	0.176	0.001	**
Grey matter volume (mm^3)	Fovea	1623.20	245.34	1652.00	298.65	8.357	> 0.001	***	0.027	0.000	0.871	
	Parafovea	1334.07	200.82	1478.12	255.51	6.149	> 0.001	***	3.167	0.037	0.081	
	Paracentral	2386.87	536.44	2686.36	448.52	1.050	0.399		5.398	0.088	0.024	*

foveal representation, and thus specific to the region of primary visual cortex that is deprived of visual input. The presence of thicker visual cortex in congenitally blind participants has been commonly attributed to aberrant pruning processes due to absent sensory input (Aguirre et al., 2017; Bourgeois et al., 1989; Guerreiro et al., 2015; Park et al., 2009; Stryker and Harris, 1986). Increased cortical thickness has also been observed in cases of later, acquired localised vision loss, but in areas adjacent to the deafferented region. In this situation, it has been proposed that cortical thickening may represent a form of cortical plasticity, as areas adjacent to the representation of the lesion are likely to be used more frequently (Burge et al., 2016). Our use of localised regions of interest clearly demonstrated that increased cortical thickness was present only in the deafferented foveal representation, supporting the previously raised notion of disrupted pruning. Several studies have also demonstrated that in congenitally blind individuals, the cortical regions with increased thickness frequently process information from other sensory modalities, commonly referred to as cross-modal plasticity (Anurova et al., 2015; Bavelier and Neville, 2002; Bedny et al., 2011; Cohen et al., 1999, 1997; Cunningham et al., 2015; Guerreiro et al., 2015; Sadato et al., 2002; Sadato et al., 1996). It is yet to be seen if the localised increase in cortical thickness found in ACHM patients is also correlated with cross-modal plasticity.

At first glance, an increase in thickness of the deafferented visual cortex might appear counterintuitive. The discrepancy in the direction of macrostructural changes has been generally attributed to different developmental trajectories of horizontal and vertical cortical dimensions (Kelly et al., 2015; Park et al., 2009; Rakic, 1995; Wierenga et al., 2014). In this respect, increased cortical thickness might be related to aberrant cortical maturation, where synaptic pruning, a process to abolish weaker cortical connections, is halted due to missing sensory input (Aguirre et al., 2017; Bourgeois et al., 1989; Guerreiro et al., 2015; Park et al., 2009; Stryker and Harris, 1986). Importantly, the standardised automated algorithm used to define cortical thickness (Fischl and Dale, 2000), is susceptible to the degree of intracortical myelination. Thus, the apparent change in cortical thickness observed may reflect differences in myelination between patients and controls (Aguirre et al., 2016; Glasser and Van Essen, 2011; Park et al., 2009). A recent study by Natu et al. (2019) indicated that the apparent thinning of the cortex over the course of normal development was correlated with an increase in myelination. Consequently, the apparent thickening observed in ACHM may reflect a failure to increase or even a decrease in cortical myelination. Our results thus lend further support to the possibility that missing sensory input can affect developmental myelination processes. Future research measuring cortical myelin in achromatopsia could shed light on this hypothesis.

4.2. Broad reduction in surface area

In the current study, we found reduced surface area in ACHM in all three central representations analysed within primary visual cortex. This was in contrast to the more localized region of cortical thickening found only in the deafferented region and indicates that loss of cone input has more widespread effects on surface area.

A decrease in overall surface area in primary visual cortex is commonly reported in early total blindness affecting the entire visual field (Aguirre et al., 2016; Noppeney et al., 2005; Pan et al., 2007; Park et al., 2009; Ptito et al., 2008). Most studies that reported changes in early blindness focused either on the whole primary visual cortex or on the pericalcarine areas (Aguirre et al., 2016; Park et al., 2009) and included participants with blindness from a variety of causes and with a variety of visual field defects. In our ACHM cohort, surface area reduction was found across the entire extent of primary visual cortex measured (0°-8°), beyond the small, localised absolute visual field defect (Baseler et al., 2002).

Surface area is known to reach a maximum later in life, around the age of nine (Mills et al., 2014; Raznahan et al., 2011). Interestingly, pericalcarine areas do not seem to follow this general trend and no age-related peak could be observed (Wierenga et al., 2014). An earlier study reported that surface area peaks shortly after birth, especially within the highly convoluted foveal representation important for central vision (Leuba and Kraftsik, 1994). These are precisely the cortical regions that are deafferented in ACHM, potentially leading to profound effects on cortical maturation. This in turn might impact on the subsequent development of more peripheral representations, possibly explaining the broader area of reduction we observed here. Moreover, while the highest cone density is found at the foveola, leading to a central absolute scotoma in ACHM, cone photoreceptors decrease in number with eccentricity, but are still fairly numerous up to an eccentricity of 15° (Curcio et al., 1991, 1990; Osterberg, 1937). Thus, the visual defect in ACHM is not limited to the foveola, supporting the possibility that the absence of cone signalling may have more widespread consequences on cortical architecture. Some recent studies also highlighted an ACHM subpopulation with compromised rod function which could be observed across all different genetic backgrounds (Khan et al., 2007; Maguire et al., 2018; Moskowitz et al., 2009; Wang et al., 2012; Zelinger et al., 2015). If this cohort also encompasses such individuals, this would also lead to a more severe reduction in surface area beyond the representation of the absolute rod scotoma.

4.3. Reduction in grey matter volume

Although an overall decrease in grey matter volume has been reported in the occipital lobes for congenital, complete blindness (Boucard et al., 2009; Bridge et al., 2009; Burge et al., 2016; Plank et al., 2011; Prins et al., 2016b), we found only a subtle reduction in grey volume outside the retinotopic presentation of the absolute scotoma in ACHM, which was the only metric that did not pass subsequent multiple testing corrections. While grey matter volume encapsulates both cortical thickness and surface area (Winkler et al., 2018; Winkler et al., 2010), it was shown that grey matter volume is generally more influenced by changes to surface area rather than cortical thickness (Aguirre et al., 2016; Winkler et al., 2018). This is supported by our data, where a reduction in grey matter volume was only evident in the paracentral representations of visual cortex where surface area was most reduced. Conversely, grey matter volume remained constant in the foveal representation, where surface area and thickness changed in opposite directions. This finding clearly highlights that without further metrics such as surface area and thickness, the true extent of changes to cortical structure might not be captured. This underlines the limited specificity of measurements restricted to cortical volume (Winkler et al., 2018).

4.4. Implications of changes to cortical microstructure for cortical remapping and prospects for current restorative approaches

At this point, it is unclear to what extent cortical changes will impact current vision restoration therapies in this patient population. For example, increased cortical thickness in individuals who were born blind remained even after the cause of blindness e.g., cataracts, was reversed. Moreover, cortical thickness was negatively correlated with visual task performance while auditory task performance was positively correlated (Guerreiro et al., 2016; Guerreiro et al., 2015). It appears therefore that the outcome of restoring vision can be explicitly linked to the way in which the visual cortex has been shaped during periods of deprivation. While increased cortical thickness and related cross-modal plasticity can be a limiting factor (Guerreiro et al., 2016, Guerreiro et al., 2015) and are therefore likely to shape the extent of the recovery, there may be some improvement. Two studies using adeno-associated virus (AAV) encoding CNGA3 in CNGA3-achromatopsia subjects (Fischer et al., 2020; McKyton et al., 2021) described subtle improvement in acuity and contrast sensitivity measurements, a reduction in photo aversion, which was accompanied by patients' reports of better, more detailed everyday vision. Furthermore, McKyton et al. (2021) described

cortical functional changes following treatment: patient population-receptive field sizes that were atypically large in early visual areas, decreased following treatment, demonstrating the ability for cortex to encode new input, even in adulthood. This shows that while cortical thickening may limit the desired therapeutic outcome, it does not entirely prevent improvements from gene therapeutic interventions.

While the underlying mechanisms of cortical thickening are not yet clear, it is known that cortical thickness is significantly and inversely related to the age of blindness onset (Li et al., 2017). Increased thickness and the link to cross-modal plasticity and its limiting effects are therefore important factors to consider. Such structural changes along with the reduction in surface area reported here suggest that early intervention might be beneficial to allow for normal cortical development in ACHM. Future clinical studies should consider including cortical thickness as a follow-up measure to better understand the promise and limits of novel restorative treatment.

4.5. Limitations and future studies

First, one clear limitation of the study is the small sample size especially when compared to studies using brain imaging data stemming from large data sets, such as the UK Biobank (Littlejohns et al., 2020; Miller et al., 2016). Nevertheless, our study includes the largest cohort of participants to date with the rare condition ACHM and not only offers valuable clinical insights but also novel entry points for further investigations. Second, while multi-centre collaborations facilitate the recruitment of participants with rare disorders, this also poses challenges arising from differences in scanner settings and protocols. While studies comparing the reliability of surface-based measures mostly report only minor differences across scanners, the largest discrepancies, especially for cortical thickness, have been found in the visual cortex (Han et al., 2006) which may in part be related to its high myelin content (Fischl and Dale, 2000; Glasser and Van Essen, 2011). We took careful precautions to remove potential biases introduced by the multi-site nature of this study by including HCs from each respective site and incorporating scanner site as a confounding variable in our statistical analysis.

In the current study, we chose to use an ROI-based analysis focusing on primary brain regions that process central vision in order to maximise sensitivity. However, it is possible that higher order visual processing regions are also affected, particularly those that rely on cone input to process colour, patterns and form/shape. A recent study compared structural differences more broadly in the dorsal and ventral visual processing pathways of the brain in ACHM, reporting a reduction in overall cortical surface area in several visual areas (V1, V2, V3, TO1, hV4, and LO1) (Lowndes et al., 2021).

While findings reported here highlight the importance of visual input during brain development and a possible benefit of earlier interventions in ACHM, we can only speculate regarding the optimal time point for gene therapeutic interventions. Longitudinal studies, especially in a younger cohort, would be a crucial next step to measure cortical changes over time and their functional and behavioural consequences in order to identify a time window for clinical intervention that ensures maximal treatment efficacy. Further, incorporating multimodal brain imaging measurements to determine changes in myelin content (Glasser and Van Essen, 2011; Natu et al., 2019) and brain neurochemistry would help to elucidate microstructural mechanisms underlying cortical changes in ACHM.

4.5.1. Conclusion

Here, we demonstrate a specific structural alteration of the primary visual cortex in ACHM that is associated with the congenital absence of input from the cone photoreceptors. Besides a substantial reduction in cortical surface area we report a highly localized thickening of cortical areas representing the fovea. Previous research has shown that thickening is experience dependent, may not be reversible and is associated with poorer visual outcomes. Our finding of a localized increase in cortical thickness shows clinical relevance in terms of potential outcomes of restorative approaches of ACHM received in adulthood. The described cortical changes point to possible benefits of future treatments in ACHM when applied earlier in life, when differences from normal cortical development are not yet present or are more easily reversed.

5. Data availability

Within the limits of privacy issues of clinical data and the need for approval from the site-specific local ethics committee, data will be made available upon request. This study used openly available software and code, namely Freesurfer analysis suite, Version 6.0 (https://surfer.nmr.mgh.harvard.edu/) and the retinotopy atlas included in the python toolbox neuropythy' (https://github.com/noahbenson/neuropythy).

CRediT authorship contribution statement

Barbara Molz: Conceptualization, Writing – original draft, Writing – review & editing. **Anne Herbik:** Conceptualization, Writing – original draft. **Heidi A. Baseler:** Conceptualization, Resources. **Pieter B. de Best:** Resources, Validation. **Richard W. Vernon:** Software. **Noa Raz:** Resources. **Andre D. Gouws:** Resources. **Khazar Ahmadi:** Resources. **Rebecca Lowndes:** Resources, Validation. **Rebecca J. McLean:** Resources. **Irene Gottlob:** Resources. **Susanne Kohl:** Resources. **Lars Choritz:** Resources. **John Maguire:** Resources. **Martin Kanowski:** Resources. **Barbara Käsmann-Kellner:** Resources. **Ilse Wieland:** Resources. **Eyal Banin:** Resources. **Netta Levin:** Conceptualization, Resources, Funding acquisition. **Michael B. Hoffmann:** Conceptualization, Resources, Funding acquisition. **Antony B. Morland:** Conceptualization, Resources, Funding acquisition.

Declaration of Competing Interest

The authors declare that they have no known competing financial interests or personal relationships that could have appeared to influence the work reported in this paper.

Acknowledgments

We thank the German patient association 'Achromatopsie Selbsthilfe e.V.' for support in participant recruitment. This project was supported by European Union's Horizon 2020 research and innovation programme under the Marie Sklodowska-Curie grant agreement (No. 641805) and the German Research Foundation (DFG, HO 2002/12-1). Richard Vernon was funded by the BBSRC (BB/P007252/1) grant awarded to ABM.

References

Aboshiha, J., Dubis, A.M., Carroll, J., Hardcastle, A.J., Michaelides, M., 2016. The cone dysfunction syndromes. Br. J. Ophthalmol. https://doi.org/10.1136/bjophthalmol-2014-306505.

Aguirre, G.K., Butt, O.H., Datta, R., Roman, A.J., Sumaroka, A., Schwartz, S.B., Cideciyan, A.V., Jacobson, S.G., 2017. Postretinal structure and function in severe congenital photoreceptor blindness caused by mutations in the GUCY2D gene. Invest. Ophthalmol. Vis. Sci. 58, 959–973. https://doi.org/10.1167/iovs.16-20413.

Aguirre, G.K., Datta, R., Benson, N.C., Prasad, S., Jacobson, S.G., Cideciyan, A.V., Bridge, H., Watkins, K.E., Butt, O.H., Dain, A.S., Brandes, L., Gennatas, E.D., 2016. Patterns of individual variation in visual pathway structure and function in the sighted and blind. PLoS ONE 11, e0164677. https://doi.org/10.1371/journal.pone.0164677.

Alfaro-Almagro, F., McCarthy, P., Afyouni, S., Andersson, J.L.R., Bastiani, M., Miller, K. L., Nichols, T.E., Smith, S.M., 2021. Confound modelling in UK Biobank brain imaging. NeuroImage 224, 117002. https://doi.org/10.1016/J.NEUROIMAGE.2020.117002.

Anurova, I., Renier, L.A., Volder, A.G.D., Carlson, S., Rauschecker, J.P., 2015. Relationship between cortical thickness and functional activation in the early blind. Cerebral Cortex (New York, NY) 25, 2035. https://doi.org/10.1093/CERCOR/BHU009.

Baseler, H.A., Brewer, A.A., Sharpe, L.T., Morland, A.B., Jaägle, H., Wandell, B.A., 2002. Reorganization of human cortical maps caused by inherited photoreceptor abnormalities. Nat. Neurosci. 5, 364–370. https://doi.org/10.1038/nn817.

Bavelier, D., Neville, H.J., 2002. Cross-modal plasticity: where and how? Nat. Rev. Neurosci. 3, 443–452. https://doi.org/10.1038/nrn848.

Bedny, M., Pascual-Leone, A., Dodell-Feder, D., Fedorenko, E., Saxe, R., 2011. Language processing in the occipital cortex of congenitally blind adults. Proc. Natl. Acad. Sci. 108, 4429–4434. https://doi.org/10.1073/pnas.1014818108.

Benson, N.C., Butt, O.H., Brainard, D.H., Aguirre, G.K., 2014. Correction of distortion in flattened representations of the cortical surface allows prediction of v1–v3 functional organization from anatomy. PLoS Comput. Biol. 10, e1003538 https://doi.org/10.1371/journal.pcbi.1003538.

Benson, N.C., Winawer, J., 2018. Bayesian analysis of retinotopic maps. eLife 7. https://doi.org/10.7554/eLife.40224.

Boucard, C.C., Hernowo, A.T., Maguire, R.P., Jansonius, N.M., Roerdink, J.B.T.M., Hooymans, J.M.M., Cornelissen, F.W., 2009. Changes in cortical grey matter density associated with long-standing retinal visual field defects. Brain 132, 1898–1906. https://doi.org/10.1093/brain/awp119.

Bourgeois, J.P., Jastreboff, P.J., Rakic, P., 1989. Synaptogenesis in visual cortex of normal and preterm monkeys: evidence for intrinsic regulation of synaptic overproduction. Proc. Natl. Acad. Sci. 86, 4297–4301. https://doi.org/10.1073/pnas.86.11.4297.

Bridge, H., Cowey, A., Ragge, N., Watkins, K.E., 2009. Imaging studies in congenital anophthalmia reveal preservation of brain architecture in "visual" cortex. Brain 132, 3467–3480. https://doi.org/10.1093/brain/awp279.

Bridge, H., von dem Hagen, E.A.H., Davies, G., Chambers, C., Gouws, A.D., Hoffmann, M. B., Morland, A.B., 2014. Changes in brain morphology in albinism reflect reduced visual acuity. Cortex 56, 64–72. https://doi.org/10.1016/j.cortex.2012.08.010.

Burge, W.K., Griffis, J.C., Nenert, R., Elkhetali, A., Decarlo, D.K., Ver Hoef, L.W., Ross, L. A., Visscher, K.M., 2016. Cortical thickness in human V1 associated with central vision loss. Sci. Rep. 6, 23268. https://doi.org/10.1038/srep23268.

Cohen, L.G., Celnik, P., Pascual-Leone, A., Corwell, B., Faiz, L., Dambrosia, J., Honda, M., Sadato, N., Gerloff, C., Dolores Catalá, M., Hallett, M., 1997. Functional relevance of cross-modal plasticity in blind humans. Nature 389, 180–183. https://doi.org/10.1038/38278.

Cohen, L.G., Weeks, R.A., Sadato, N., Celnik, P., Ishii, K., Hallett, M., 1999. Period of susceptibility for cross-modal plasticity in the blind. Ann. Neurol. 45, 451–460.

Cunningham, S.I., Weiland, J.D., Bao, P., Lopez-Jaime, G.R., Tjan, B.S., 2015. Correlation of vision loss with tactile-evoked V1 responses in retinitis pigmentosa. Vision Res. 111, 197–207. https://doi.org/10.1016/j.visres.2014.10.015.

Curcio, C.A., Allen, K.A., Sloan, K.R., Lerea, C.L., Hurley, J.B., Klock, I.B., Milam, A.H., 1991. Distribution and morphology of human cone photoreceptors stained with anti-blue opsin. J. Compar. Neurol. 312, 610–624. https://doi.org/10.1002/cne.903120411.

Curcio, C.A., Sloan, K.R., Kalina, R.E., Hendrickson, A.E., 1990. Human photoreceptor topography. J. Compar. Neurol. 292, 497–523. https://doi.org/10.1002/cne.902920402.

d'Almeida, O.C., Mateus, C., Reis, A., Grazina, M.M., Castelo-Branco, M., 2013. Long term cortical plasticity in visual retinotopic areas in humans with silent retinal ganglion cell loss. NeuroImage 81, 222–230. https://doi.org/10.1016/j.neuroimage.2013.05.032.

Dale, A.M., Fischl, B., Sereno, M.I., 1999. Cortical surface-based analysis: I Segmentation and surface reconstruction. NeuroImage 9, 179–194. https://doi.org/10.1006/nimg.1998.0395.

Desikan, R.S., Ségonne, F., Fischl, B., Quinn, B.T., Dickerson, B.C., Blacker, D., Buckner, R.L., Dale, A.M., Maguire, R.P., Hyman, B.T., Albert, M.S., Killiany, R.J., 2006. An automated labeling system for subdividing the human cerebral cortex on MRI scans into gyral based regions of interest. NeuroImage 31, 968–980. https://doi.org/10.1016/j.neuroimage.2006.01.021.

Fischer, M.D., Michalakis, S., Wilhelm, B., Zobor, D., Muehlfriedel, R., Kohl, S., Weisschuh, N., Ochakovski, G.A., Klein, R., Schoen, C., Sothilingam, V., Garcia-Garrido, M., Kuehlewein, L., Kahle, N., Werner, A., Dauletbekov, D., Paquet-Durand, F., Tsang, S., Martus, P., Peters, T., Seeliger, M., Bartz-Schmidt, K.U., Ueffing, M., Zrenner, E., Biel, M., Wissinger, B., 2020. Safety and vision outcomes of subretinal gene therapy targeting cone photoreceptors in achromatopsia: a nonrandomized controlled trial. JAMA Ophthalmol. 138, 643–651. https://doi.org/10.1001/jamaophthalmol.2020.1032.

Fischl, B., Dale, A.M., 2000. Measuring the thickness of the human cerebral cortex from magnetic resonance images. PNAS 97, 11050–11055. https://doi.org/10.1073/pnas.200033797.

Fischl, B., Sereno, M.I., Dale, A.M., 1999. Cortical surface-based analysis: II. Inflation, flattening, and a surface-based coordinate system. NeuroImage 9, 195–207. https://doi.org/10.1006/nimg.1998.0396.

Fischl, B., Van Der Kouwe, A., Destrieux, C., Halgren, E., Ségonne, F., Salat, D.H., Busa, E., Seidman, L.J., Goldstein, J., Kennedy, D., Caviness, V., Makris, N., Rosen, B., Dale, A.M., 2004. Automatically parcellating the human cerebral cortex. Cereb. Cortex 14, 11–22. https://doi.org/10.1093/cercor/bhg087.

Glasser, M.F., Van Essen, D.C., 2011. Mapping human cortical areas in vivo based on myelin content as revealed by T1- and T2-weighted MRI. J. Neurosci. 31, 11597–11616. https://doi.org/10.1523/jneurosci.2180-11.2011.

Guerreiro, M.J.S., Erfort, M.V., Henssler, J., Putzar, L., Röder, B., 2015. Increased visual cortical thickness in sight-recovery individuals. Hum. Brain Mapp. 36, 5265–5274. https://doi.org/10.1002/hbm.23009.

Guerreiro, M.J.S., Putzar, L., Röder, B., 2016. Persisting cross-modal changes in sight-recovery individuals modulate visual perception. Curr. Biol. 26, 3096–3100. https://doi.org/10.1016/j.cub.2016.08.069.

Haegerstrom-Portnoy, G., Schneck, M.E., Verdon, W.A., Hewlett, S.E., 1996. Clinical vision characteristics of the congenital achromatopsias. II Color vision. Optomet. Vision Sci. 73, 457–465. https://doi.org/10.1097/00006324-199607000-00002.

Han, X., Jovicich, J., Salat, D.H., van der Kouwe, A., Quinn, B.T., Czanner, S., Busa, E., Pacheco, J., Albert, M.S., Killiany, R.J., Maguire, P., Rosas, D., Makris, N., Dale, A. M., Dickerson, B., Fischl, B., 2006. Reliability of MRI-derived measurements of human cerebral cortical thickness: the effects of field strength, scanner upgrade and manufacturer. NeuroImage 32, 180–194. https://doi.org/10.1016/j.neuroimage.2006.02.051.

Hirji, N., Georgiou, M., Kalitzeos, A., Bainbridge, J.W., Kumaran, N., Aboshiha, J., Carroll, J., Michaelides, M., 2018. Longitudinal assessment of retinal structure in achromatopsia patients with long-term follow-up. Invest. Ophthalmol. Vis. Sci. 59, 5735–5744. https://doi.org/10.1167/iovs.18-25452.

Holm, S., 1979. A simple sequentially rejective multiple test procedure. Scand. J. Stat. 6, 65–70.

Jiang, J., Zhu, W., Shi, F., Liu, Y., Li, J., Qin, W., Li, K., Yu, C., Jiang, T., 2009. Thick visual cortex in the early blind. J. Neurosci. 29, 2205–2211. https://doi.org/10.1523/JNEUROSCI.5451-08.2009.

Kelly, K.R., Desimone, K.D., Gallie, B.L., Steeves, J.K.E., 2015. Increased cortical surface area and gyrification following long-term survival from early monocular enucleation. NeuroImage: Clinical 7, 297–305. https://doi.org/10.1016/j.nicl.2014.11.020.

Khan, N.W., Wissinger, B., Kohl, S., Sieving, P.A., 2007. CNGB3 achromatopsia with progressive loss of residual cone function and impaired rod-mediated function. Invest. Ophthalmol. Vis. Sci. 48, 3864–3871. https://doi.org/10.1167/iovs.06-1521.

Lemos, J., Pereira, D., Castelo-Branco, M., 2016. Visual cortex plasticity following peripheral damage to the visual system: fMRI evidence. Curr. Neurol. Neurosci. Rep. https://doi.org/10.1007/s11910-016-0691-0.

Leuba, G., Kraftsik, R., 1994. Changes in volume, surface estimate, three-dimensional shape and total number of neurons of the human primary visual cortex from midgestation until old age. Anat. Embryol. 190, 351–366. https://doi.org/10.1007/BF00187293.

Li, Q., Song, M., Xu, J., Qin, W., Yu, C., Jiang, T., 2017. Cortical thickness development of human primary visual cortex related to the age of blindness onset. Brain Imag. Behav. 11, 1029–1036. https://doi.org/10.1007/s11682-016-9576-8.

Littlejohns, T.J., Holliday, J., Gibson, L.M., Garratt, S., Oesingmann, N., Alfaro-Almagro, F., Bell, J.D., Boultwood, C., Collins, R., Conroy, M.C., Crabtree, N., Doherty, N., Frangi, A.F., Harvey, N.C., Leeson, P., Miller, K.L., Neubauer, S., Petersen, S.E., Sellors, J., Sheard, S., Smith, S.M., Sudlow, C.L.M., Matthews, P.M., Allen, N.E., 2020. The UK Biobank imaging enhancement of 100,000 participants: rationale, data collection, management and future directions. Nature Communications 2020 11:1 11, 1–12. https://doi.org/10.1038/s41467-020-15948-9.

Lowndes, R., Molz, B., Warriner, L., Herbik, A., de Best, P.B., Raz, N., Gouws, A., Ahmadi, K., McLean, R.J., Gottlob, I., Kohl, S., Choritz, L., Maguire, J., Kanowski, M., Käsmann-Kellner, B., Wieland, I., Banin, E., Levin, N., Hoffmann, M.B., Morland, A. B., Baseler, H.A., 2021. Structural differences across multiple visual cortical regions in the absence of cone function in congenital achromatopsia. Front. Neurosci. 2021 https://doi.org/10.3389/fnins.2021.718958.

Maguire, J., McKibbin, M., Khan, K., Kohl, S., Ali, M., McKeefry, D.J., 2018. CNGB3 mutations cause severe rod dysfunction. Ophthalmic Genet. 39, 108–114. https://doi.org/10.1080/13816810.2017.1368087.

McCulloch, D.L., Marmor, M.F., Brigell, M.G., Hamilton, R., Holder, G.E., Tzekov, R., Bach, M., 2015. ISCEV Standard for full-field clinical electroretinography (2015 update). Documenta ophthalmologica. Adv. Ophthalmol. 130, 1–12. https://doi.org/10.1007/s10633-014-9473-7.

McKyton, A., Averbukh, E., Ohana, D.M., Levin, N., Banin, E., 2021. Cortical visual mapping following ocular gene augmentation therapy for achromatopsia. J. Neurosci. 41, 7363–7371. https://doi.org/10.1523/JNEUROSCI.3222-20.2021.

Michalakis, S., Schön, C., Becirovic, E., Biel, M., 2017. Gene therapy for achromatopsia. J. Gene Med. https://doi.org/10.1002/jgm.2944.

Miller, K.L., Alfaro-Almagro, F., Bangerter, N.K., Thomas, D.L., Yacoub, E., Xu, J., Bartsch, A.J., Jbabdi, S., Sotiropoulos, S.N., Andersson, J.L.R., Griffanti, L., Douaud, G., Okell, T.W., Weale, P., Dragonu, I., Garratt, S., Hudson, S., Collins, R., Jenkinson, M., Matthews, P.M., Smith, S.M., 2016. Multimodal population brain imaging in the UK Biobank prospective epidemiological study. Nature Neuroscience 2016 19:11 19, 1523–1536. https://doi.org/10.1038/nn.4393.

Mills, K.L., Lalonde, F., Clasen, L.S., Giedd, J.N., Blakemore, S.J., 2014. Developmental changes in the structure of the social brain in late childhood and adolescence. Soc. Cognit. Affect. Neurosci. 9, 123–131. https://doi.org/10.1093/scan/nss113.

Moskowitz, A., Hansen, R.M., Akula, J.D., Eklund, S.E., Fulton, A.B., 2009. Rod and rod-driven function in achromatopsia and blue cone monochromatism. Invest. Ophthalmol. Vis. Sci. 50, 950–958. https://doi.org/10.1167/iovs.08-2544.

Natu, V.S., Gomez, J., Barnett, M., Jeska, B., Kirilina, E., Jaeger, C., Zhen, Z., Cox, S., Weiner, K.S., Weiskopf, N., Grill-Spector, K., 2019. Apparent thinning of human visual cortex during childhood is associated with myelination. PNAS 116, 20750–20759. https://doi.org/10.1073/pnas.1904931116.

Noppeney, U., Friston, K.J., Ashburner, J., Frackowiak, R., Price, C.J., 2005. Early visual deprivation induces structural plasticity in gray and white matter [1]. Curr. Biol. https://doi.org/10.1016/j.cub.2005.06.053.

Osterberg, G., 1937. Topography of the layer of rods and cones in the human retina. J. Am. Med. Assoc. 108, 232. https://doi.org/10.1001/jama.1937.02780030070033.

Pan, W.J., Wu, G., Li, C.X., Lin, F., Sun, J., Lei, H., 2007. Progressive atrophy in the optic pathway and visual cortex of early blind Chinese adults: a voxel-based morphometry magnetic resonance imaging study. NeuroImage 37, 212–220. https://doi.org/10.1016/j.neuroimage.2007.05.014.

Park, H.J., Lee, J.D., Kim, E.Y., Park, B., Oh, M.K., Lee, S.C., Kim, J.J., 2009. Morphological alterations in the congenital blind based on the analysis of cortical thickness and surface area. NeuroImage 47, 98–106. https://doi.org/10.1016/j.neuroimage.2009.03.076.

Plank, T., Frolo, J., Brandl-Rühle, S., Renner, A.B., Hufendiek, K., Helbig, H., Greenlee, M.W., 2011. Gray matter alterations in visual cortex of patients with loss of central vision due to hereditary retinal dystrophies. NeuroImage 56, 1556–1565. https://doi.org/10.1016/j.neuroimage.2011.02.055.

Prins, D., Hanekamp, S., Cornelissen, F.W., 2016a. Structural brain MRI studies in eye diseases: Are they clinically relevant? A review of current findings. Acta Ophthalmologica. https://doi.org/10.1111/aos.12825.

Prins, D., Plank, T., Baseler, H.A., Gouws, A.D., Beer, A., Morland, A.B., Greenlee, M.W., Cornelissen, F.W., 2016b. Surface-based analyses of anatomical properties of the visual cortex in macular degeneration. PLoS ONE 11, e0146684. https://doi.org/10.1371/journal.pone.0146684.

Ptito, M., Schneider, F.C.G., Paulson, O.B., Kupers, R., 2008. Alterations of the visual pathways in congenital blindness. Exp. Brain Res. 187, 41–49. https://doi.org/10.1007/s00221-008-1273-4.

Rakic, P., 1995. A small step for the cell, a giant leap for mankind: a hypothesis of neocortical expansion during evolution. Trends Neurosci. 18, 383–388. https://doi.org/10.1016/0166-2236(95)93934-P.

Raznahan, A., Shaw, P., Lalonde, F., Stockman, M., Wallace, G.L., Greenstein, D., Clasen, L., Gogtay, N., Giedd, J.N., 2011. How does your cortex grow? J. Neurosci. 31, 7174–7177. https://doi.org/10.1523/JNEUROSCI.0054-11.2011.

Remmer, M.H., Rastogi, N., Ranka, M.P., Ceisler, E.J., 2015. Achromatopsia: a review. Curr. Opin. Ophthalmol. https://doi.org/10.1097/ICU.0000000000000189.

Sadato, N., Okada, T., Honda, M., Yonekura, Y., 2002. Critical period for cross-modal plasticity in blind humans: a functional MRI study. NeuroImage 16, 389–400. https://doi.org/10.1006/nimg.2002.1111.

Sadato, N., Pascual-Leone, A., Grafman, J., Ibañez, V., Deiber, M.P., Dold, G., Hallett, M., 1996. Activation of the primary visual cortex by Braille reading in blind subjects. Nature 380, 526–528. https://doi.org/10.1038/380526a0.

Ségonne, F., Dale, A.M., Busa, E., Glessner, M., Salat, D.H., Hahn, H.K., Fischl, B., 2004. A hybrid approach to the skull stripping problem in MRI. NeuroImage 22, 1060–1075. https://doi.org/10.1016/j.neuroimage.2004.03.032.

Sled, J.G., Zijdenbos, A.P., Evans, A.C., 1998. A nonparametric method for automatic correction of intensity nonuniformity in MRI data. IEEE Trans. Med. Imaging 17, 87–97. https://doi.org/10.1109/42.668698.

Stryker, M.P., Harris, W.A., 1986. Binocular impulse blockade prevents the formation of ocular dominance columns in cat visual cortex. J. Neurosci. Off. J. Soc. Neurosci. 6, 2117–2133.

Von Dem Hagen, E.A.H., Houston, G.C., Hoffmann, M.B., Jeffery, G., Morland, A.B., 2005. Retinal abnormalities in human albinism translate into a reduction of grey matter in the occipital cortex. Eur. J. Neurosci. 22, 2475–2480. https://doi.org/10.1111/j.1460-9568.2005.04433.x.

Wang, I., Khan, N.W., Branham, K., Wissinger, B., Kohl, S., Heckenlively, J.R., 2012. Establishing baseline rod electroretinogram values in achromatopsia and cone dystrophy. Doc. Ophthalmol. 125, 229–233. https://doi.org/10.1007/s10633-012-9350-1.

Wierenga, L.M., Langen, M., Oranje, B., Durston, S., 2014. Unique developmental trajectories of cortical thickness and surface area. NeuroImage 87, 120–126. https://doi.org/10.1016/j.neuroimage.2013.11.010.

Winkler, A.M., Greve, D.N., Bjuland, K.J., Nichols, T.E., Sabuncu, M.R., Håberg, A.K., Skranes, J., Rimol, L.M., 2018. Joint analysis of cortical area and thickness as a replacement for the analysis of the volume of the cerebral cortex. Cereb. Cortex 28, 738–749. https://doi.org/10.1093/cercor/bhx308.

Winkler, A.M., Kochunov, P., Blangero, J., Almasy, L., Zilles, K., Fox, P.T., Duggirala, R., Glahn, D.C., 2010. Cortical thickness or grey matter volume? The importance of selecting the phenotype for imaging genetics studies. NeuroImage 53, 1135–1146. https://doi.org/10.1016/j.neuroimage.2009.12.028.

Zelinger, L., Cideciyan, A.V., Kohl, S., Schwartz, S.B., Rosenmann, A., Eli, D., Sumaroka, A., Roman, A.J., Luo, X., Brown, C., Rosin, B., Blumenfeld, A., Wissinger, B., Jacobson, S.G., Banin, E., Sharon, D., 2015. Genetics and disease expression in the CNGA3 form of achromatopsia: Steps on the path to gene therapy. Ophthalmology 122, 997–1007. https://doi.org/10.1016/j.ophtha.2014.11.025.

Zobor, D., Zobor, G., Kohl, S., 2015. Achromatopsia: on the doorstep of a possible therapy. Ophthalmic Res. https://doi.org/10.1159/000435957.